Supporting Information

Quantitative Structure-Reactivity Modeling of Copper-Catalyzed Atom Transfer Radical Polymerization

Fabio di Lena and Christina L. L. Chai*

Institute of Chemical and Engineering Sciences, Agency of Science, Technology and Research, 1 Pesek Road, Jurong Island, 627833 Singapore

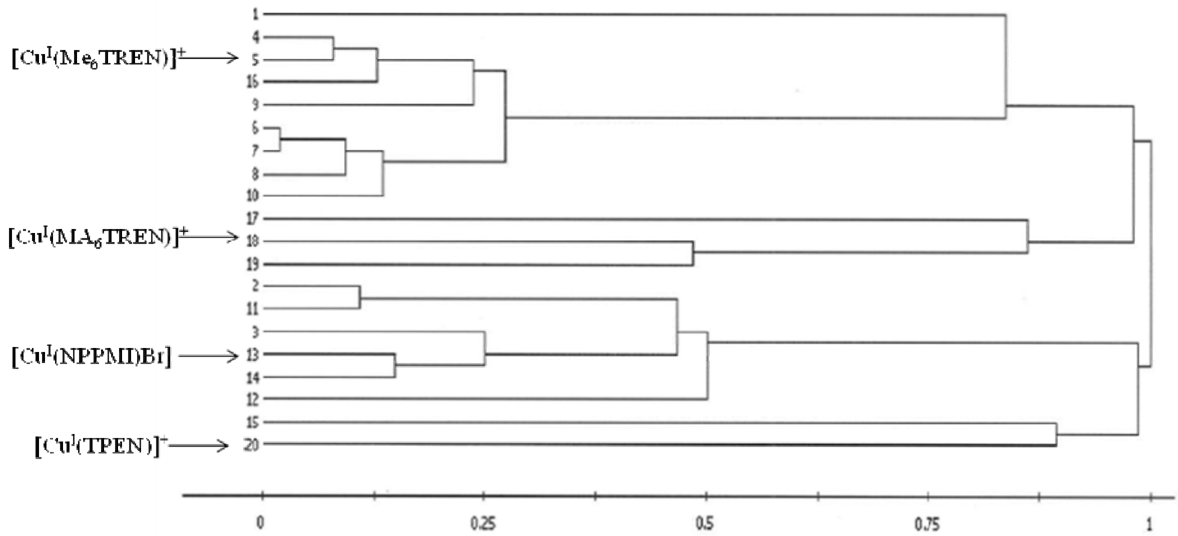

Figure 1S. Dendrogram resulting from HCA carried out on the first 6 principal components obtained by subjecting the molecular descriptors of Cu(I) complexes to PCA.

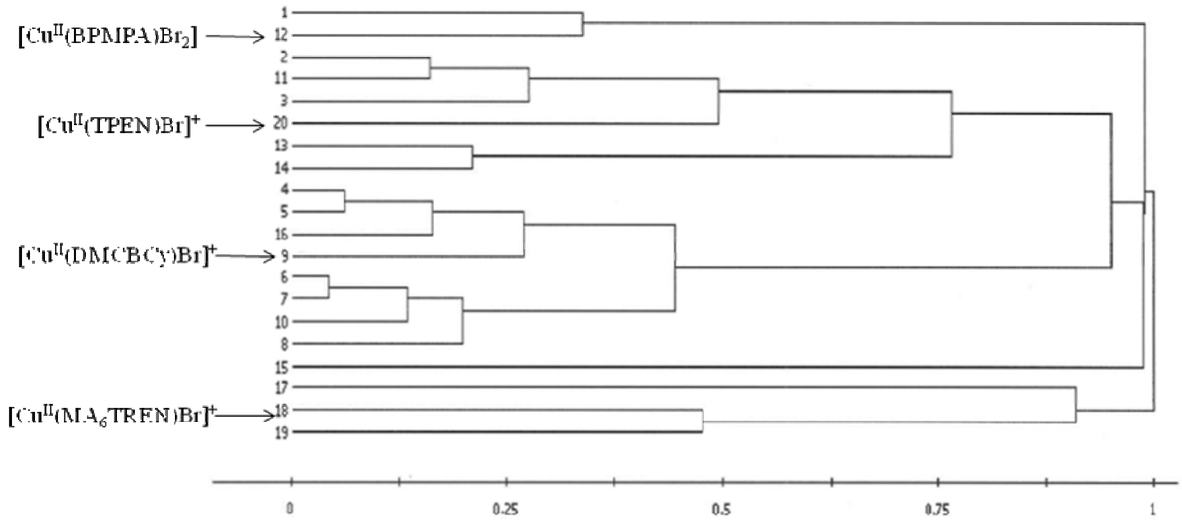

Figure 2S. Dendrogram resulting from HCA carried out on the first 6 principal components obtained by subjecting the molecular descriptors of Cu(II) complexes to PCA.

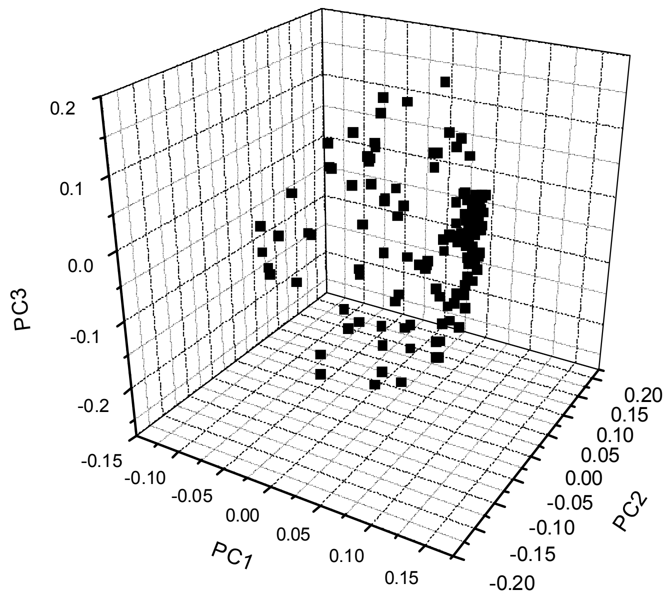

Figure 3S. Loading plot PC1 *vs.* PC2 *vs.* PC3 for the molecular descriptors of Cu(I) complexes.

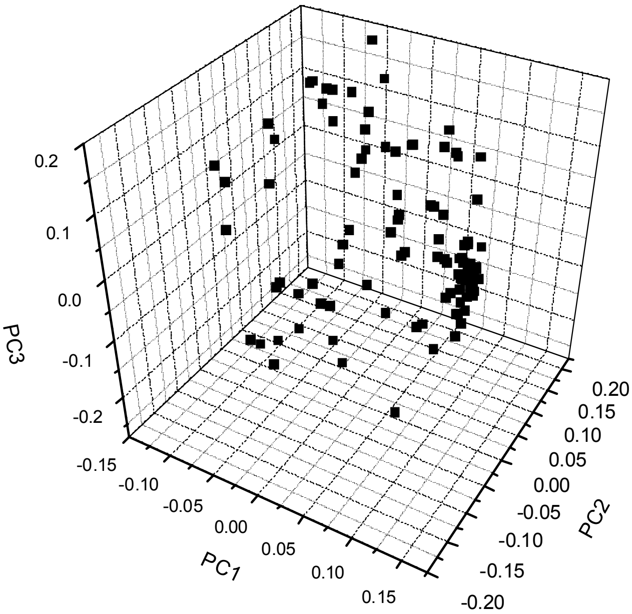

Figure 4S. Loading plot PC1 *vs.* PC2 *vs.* PC3 for the molecular descriptors of Cu(II) complexes.

	Model	Friedman's LOF	R^2	Adjusted R^2	Cross-validated R^2	SOR *F*-value	Critical SOR *F*-value (95%)
1S	$\log(k_{act}) = 3.2\times10^{-4}(\langle I_Z\text{-}5.6\times10^2\rangle) - 72(\langle\text{-}0.14\text{-HOMO}\rangle) + 5.5\times10^{-3}(\langle 3.0\times10^3\text{-CV}\rangle) + 0.60(\langle 6.5\text{-}{}^5\chi_{path}\rangle) - 1.2(\langle 6.9\text{-}{}^6\chi_{path}\rangle) + 38\times10^{-3}$	38.5×10^{-3}	0.999	0.997	0.995	793	3.51
2S	$\log(k_{act}) = 3.2\times10^{-4}(\langle I_Z\text{-}5.6\times10^2\rangle) - 72(\langle\text{-}0.14\text{-HOMO}\rangle) + 5.5\times10^{-3}(\langle 3.0\times10^3\text{-CV}\rangle) + 0.60(\langle 6.5\text{-}{}^5\chi_{path}\rangle) - 1.2(\langle 6.9\text{-}{}^6\chi_{path}\rangle) + 44\times10^{-3}$	38.8×10^{-3}	0.998	0.997	0.995	787	3.51

3S	$\log(k_{act}) = 3.2\times10^{-4}(\langle I_Z-5.6\times10^{2}\rangle) - 73(\langle -0.14-\mathrm{HOMO}\rangle) + 5.5\times10^{-3}(\langle 3.0\times10^{3}-\mathrm{CV}\rangle) + 0.60(\langle 6.6-{}^{5}\chi_{path}\rangle) - 1.2(\langle 6.9-{}^{6}\chi_{path}\rangle) + 47\times10^{-3}$	39.0×10^{-3}	0.998	0.997	0.995	784	3.51
4S	$\log(k_{act}) = - 74(\langle -0.14-\mathrm{HOMO}\rangle) - 3.6\times10^{-4}(\langle 7.2\times10^{3}-\mathrm{CV}\rangle) + 5.8\times10^{-3}(\langle 3.0\times10^{3}-\mathrm{CV}\rangle) + 0.62(\langle 6.5-{}^{5}\chi_{path}\rangle) - 1.2(\langle 6.8-{}^{6}\chi_{path}\rangle) + 1.3$	41.0×10^{-3}	0.998	0.997	0.994	745	3.51
5S	$\log(k_{act}) = 0.86(\langle {}^{6}\chi^{v}{}_{path}-4.7\rangle) - 70(\langle -0.14-\mathrm{HOMO}\rangle) + 5.4\times10^{-3}(\langle 3.0\times10^{3}-\mathrm{CV}\rangle) + 0.61(\langle 6.6-{}^{5}\chi_{path}\rangle) - 1.2(\langle 6.8-{}^{6}\chi_{path}\rangle) - 38\times10^{-3}$	41.3×10^{-3}	0.998	0.997	0.995	740	3.51
6S	$\log(k_{act}) = 3.3\times10^{-4}(\langle I_Z-8.2\times10^{2}\rangle) - 71(\langle -0.14-\mathrm{HOMO}\rangle) + 5.4\times10^{-3}(\langle 3.0\times10^{3}-\mathrm{CV}\rangle) + 0.61(\langle 6.6-{}^{5}\chi_{path}\rangle) - 1.2(\langle 6.9-{}^{6}\chi_{path}\rangle) - 38\times10^{-3}$	41.7×10^{-3}	0.998	0.997	0.995	733	3.51
7S	$\log(k_{act}) = 3.3\times10^{-4}(\langle I_Z-8.2\times10^{2}\rangle) - 72(\langle -0.14-\mathrm{HOMO}\rangle) + 5.4\times10^{-3}(\langle 3.0\times10^{3}-\mathrm{CV}\rangle) + 0.61(\langle 6.5-{}^{5}\chi_{path}\rangle) - 1.2(\langle 6.9-{}^{6}\chi_{path}\rangle) + 67\times10^{-3}$	42.2×10^{-3}	0.998	0.997	0.995	725	3.51
8S	$\log(k_{act}) = 6.8\times10^{-4}(\langle I_Z-3.0\times10^{3}\rangle) - 68(\langle -0.14-\mathrm{HOMO}\rangle) + 5.8\times10^{-3}(\langle 2.9\times10^{3}-\mathrm{CV}\rangle) + 0.57(\langle 6.6-{}^{5}\chi_{path}\rangle) - 1.2(\langle 6.9-{}^{6}\chi_{path}\rangle) + 0.18$	42.9×10^{-3}	0.998	0.997	0.990	712	3.51
9S	$\log(k_{act}) = 6.9\times10^{-4}(\langle I_Z-3.0\times10^{3}\rangle) - 68(\langle -0.14-\mathrm{HOMO}\rangle) + 5.8\times10^{-3}(\langle 2.9\times10^{3}-\mathrm{CV}\rangle) + 0.57(\langle 6.6-{}^{5}\chi_{path}\rangle) - 1.2(\langle 6.9-{}^{6}\chi_{path}\rangle) + 0.18$	43.0×10^{-3}	0.998	0.997	0.990	710	3.51
10S	$\log(k_{act}) = 0.95(\langle {}^{6}\chi^{v}{}_{path}-5.0\rangle) - 69(\langle -0.14-\mathrm{HOMO}\rangle) + 5.8\times10^{-3}(\langle 3.0\times10^{3}-\mathrm{CV}\rangle) + 0.56(\langle 6.6-{}^{5}\chi_{path}\rangle) - 1.2(\langle 6.9-{}^{6}\chi_{path}\rangle) + 0.12$	43.0×10^{-3}	0.998	0.997	0.991	710	3.51

Table 1S. Top 10 models and relative statistical analysis for log(k_{act}) of Cu(I) activators obtained with genetic function approximation algorithm with linear splines. The models are in order of increasing Friedman's LOF values.

	Model	Friedman's LOF	R^2	Adjusted R^2	Cross-validated R^2	SOR *F*-value	Critical SOR *F*-value (95%)
11S	log(k_{deact}) = 82×10^{-3}(EE) - 12×10^{-3}(❬EE-1.7×10^{2}❭) + 77×10^{-3}(❬EE-7.7×10^{2}❭) + 4.3×10^{3}(❬L-H-5.2×10^{-3}❭) - 4.1×10^{3}(❬L-H-4.7×10^{-3}❭) + 0.47(❬$^{5}\chi^{v}_{path/cluster}$-25❭) + 0.48(❬8.3-$^{4}\chi^{v}_{path}$❭) - 53	18.0×10^{-3}	0.998	0.997	0.994	701	3.51
12S	log(k_{deact}) = 82×10^{-3}(❬EE+4.0×10^{2}❭) - 13×10^{-3}(❬EE-1.7×10^{2}❭) + 76×10^{-3}(❬7.7×10^{2}-EE❭) + 4.5×10^{3}(❬L-H-5.2×10^{-3}❭) - 4.2×10^{3}(❬L-H-4.7×10^{-3}❭) + 0.46(❬$^{5}\chi^{v}_{path/cluster}$-25❭) + 0.48(❬8.3-$^{4}\chi^{v}_{path}$❭) - 85	19.0×10^{-3}	0.998	0.997	0.990	662	3.51
13S	log(k_{deact}) = 73×10^{-3}(EE) - 12×10^{-3}(❬1.7×10^{2}-EE❭) + 80×10^{-3}(❬7.7×10^{2}-EE❭) + 3.9×10^{3}(❬L-H-5.3×10^{-3}❭) - 3.7×10^{3}(❬L-H-4.7×10^{-3}❭) + 0.44(❬$^{5}\chi^{v}_{path/cluster}$-25❭) + 0.46(❬8.4-$^{4}\chi^{v}_{path}$❭) - 53	20.8×10^{-3}	0.998	0.996	0.993	605	3.51
14S	log(k_{deact}) = 67×10^{-3}(EE) - 12×10^{-3}(❬1.7×10^{2}-EE❭) + 74×10^{-3}(❬7.7×10^{2}-EE❭) + 4.0×10^{3}(❬L-H-5.3×10^{-3}❭) - 3.8×10^{3}(❬L-H-4.7×10^{-3}❭) + 0.44(❬$^{5}\chi^{v}_{path/cluster}$-25❭) +	21.9×10^{-3}	0.998	0.996	0.993	576	3.51

	$0.49(\langle 8.3-{}^{4}\chi^{v}_{path}\rangle) - 48$							
15S	$\log(k_{deact}) = 64\times10^{-3}(\langle EE+4.0\times10^{2}\rangle) - 13\times10^{-3}(\langle 1.7\times10^{2}-EE\rangle) + 71\times10^{-3}(\langle 7.7\times10^{2}-EE\rangle) + 4.0\times10^{3}(\langle L\text{-}H-5.3\times10^{-3}\rangle) - 3.8\times10^{3}(\langle L\text{-}H-4.7\times10^{-3}\rangle) + 0.41(\langle {}^{5}\chi^{v}_{path/cluster}-24\rangle) + 0.46(\langle 8.4-{}^{4}\chi^{v}_{path}\rangle) - 72$	24.0×10^{-3}	0.998	0.996	0.990	524	3.51
16S	$\log(k_{deact}) = 62\times10^{-3}(EE) - 13\times10^{-3}(\langle 1.6\times10^{2}-EE\rangle) + 69\times10^{-3}(\langle 7.7\times10^{2}-EE\rangle) + 4.0\times10^{3}(\langle L\text{-}H-5.3\times10^{-3}\rangle) - 3.8\times10^{3}(\langle L\text{-}H-4.7\times10^{-3}\rangle) + 0.45(\langle {}^{5}\chi^{v}_{path/cluster}-25\rangle) + 0.46(\langle 8.4-{}^{4}\chi^{v}_{path}\rangle) - 44$	24.5×10^{-3}	0.998	0.996	0.991	514	3.51
17S	$\log(k_{deact}) = 73\times10^{-3}(\langle EE+4.0\times10^{2}\rangle) - 12\times10^{-3}(\langle 1.7\times10^{2}-EE\rangle) + 79\times10^{-3}(\langle 7.7\times10^{2}-EE\rangle) + 3.9\times10^{3}(\langle L\text{-}H-5.3\times10^{-3}\rangle) - 3.7\times10^{3}(\langle L\text{-}H-4.7\times10^{-3}\rangle) + 0.41(\langle {}^{5}\chi^{v}_{path/cluster}-25\rangle) + 0.46(\langle 8.4-{}^{4}\chi^{v}_{path}\rangle) - 82$	25.4×10^{-3}	0.998	0.996	0.991	495	3.51
18S	$\log(k_{deact}) = 61\times10^{-3}(\langle EE+4.0\times10^{2}\rangle) - 13\times10^{-3}(\langle 1.7\times10^{2}-EE\rangle) + 68\times10^{-3}(\langle 7.7\times10^{2}-EE\rangle) + 4.0\times10^{3}(\langle L\text{-}H-5.3\times10^{-3}\rangle) - 3.8\times10^{3}(\langle L\text{-}H-4.7\times10^{-3}\rangle) + 0.41(\langle {}^{5}\chi^{v}_{path/cluster}-25\rangle) + 0.46(\langle 8.4-{}^{4}\chi^{v}_{path}\rangle) - 69$	26.0×10^{-3}	0.998	0.995	0.991	486	3.51
19S	$\log(k_{deact}) = 94\times10^{-3}(\langle EE+3.7\times10^{2}\rangle) - 15\times10^{-3}(\langle EE-1.4\times10^{2}\rangle) + 86\times10^{-3}(\langle 7.8\times10^{2}-EE\rangle) + 1.3\times10^{4}(\langle L\text{-}H-5.3\times10^{-3}\rangle) - 1.3\times10^{4}(\langle L\text{-}H-5.2\times10^{-3}\rangle) + 0.26(\langle {}^{5}\chi^{v}_{path/cluster}-23\rangle) + 0.58(\langle 7.8-{}^{4}\chi^{v}_{path}\rangle) - 95$	27.8×10^{-3}	0.997	0.995	0.991	453	3.51

20S	$\log(k_{deact}) = 90\times10^{-3}(\langle EE+4.0\times10^{2}\rangle) - 12\times10^{-3}(\langle EE-1.8\times10^{2}\rangle) + 85\times10^{-3}(\langle 7.7\times10^{2}-EE\rangle) + 5.0\times10^{3}(\langle L\text{-}H-5.2\times10^{-3}\rangle) - 4.8\times10^{3}(\langle L\text{-}H-4.7\times10^{-3}\rangle) + 0.48(\langle {}^{5}\chi^{v}_{path/cluster}-26\rangle) + 0.57(\langle 7.8-{}^{4}\chi^{v}_{path}\rangle) - 95$	28.6×10^{-3}	0.997	0.995	0.972	441	3.51

Table 2S. Top 10 models and relative statistical analysis for $\log(k_{deact})$ of Cu(II) deactivators obtained with genetic function approximation algorithm with linear splines. The models are in order of increasing Friedman's LOF values.

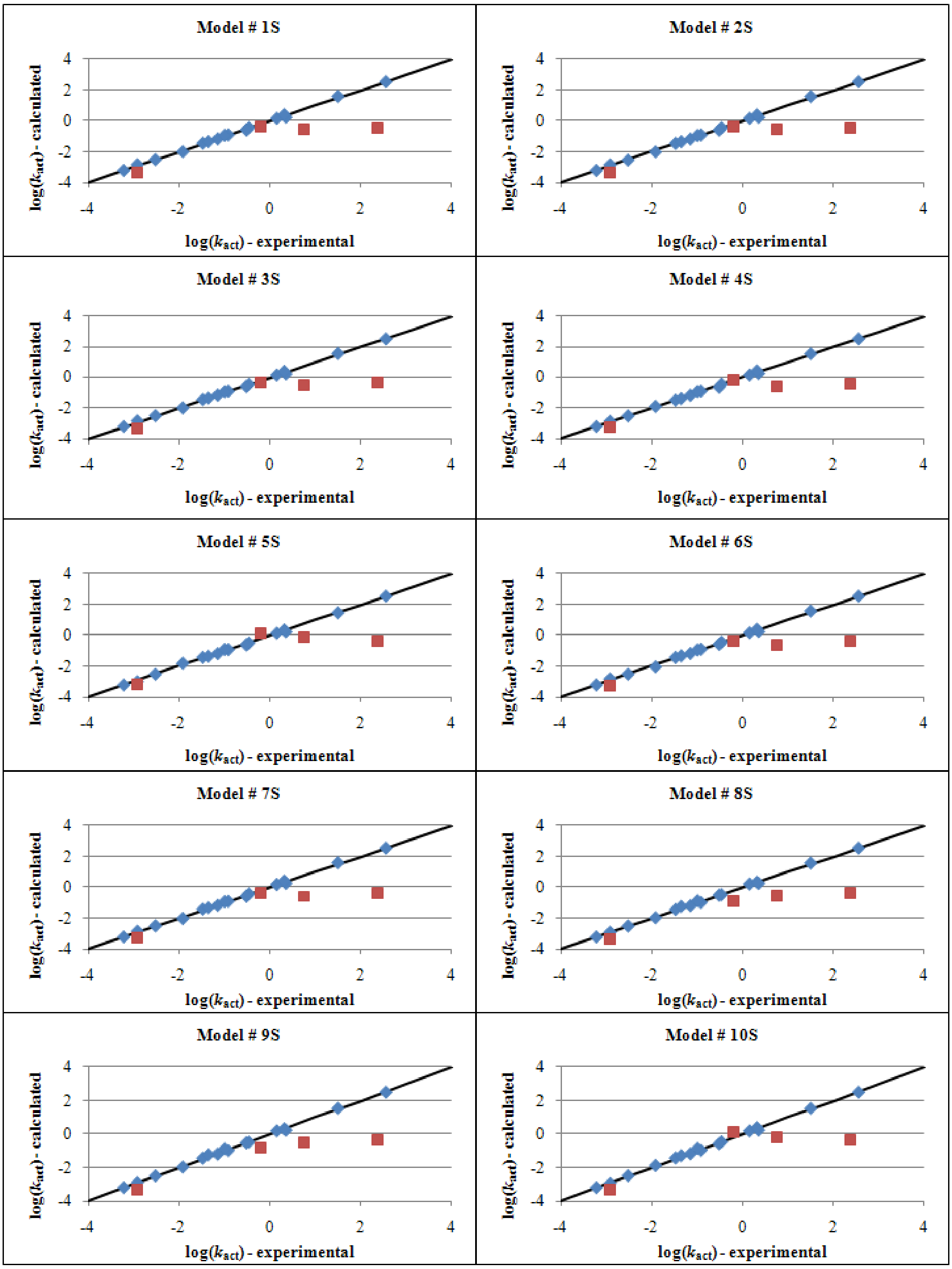
Model # 1S
log(kact) - calculated
log(kact) - experimental
Model # 2S
log(kact) - calculated
log(kact) - experimental
Model # 3S
log(kact) - calculated
log(kact) - experimental
Model # 4S
log(kact) - calculated
log(kact) - experimental
Model # 5S
log(kact) - calculated
log(kact) - experimental
Model # 6S
log(kact) - calculated
log(kact) - experimental
Model # 7S
log(kact) - calculated
log(kact) - experimental
Model # 8S
log(kact) - calculated
log(kact) - experimental
Model # 9S
log(kact) - calculated
log(kact) - experimental
Model # 10S
log(kact) - calculated
log(kact) - experimental

Figure 5S. Calculated *vs*. experimental log(k_{act}) values for Cu(I) activators obtained by genetic function approximation analysis with linear splines. Training and test sets are represented by the symbols "♦" and "■", respectively.

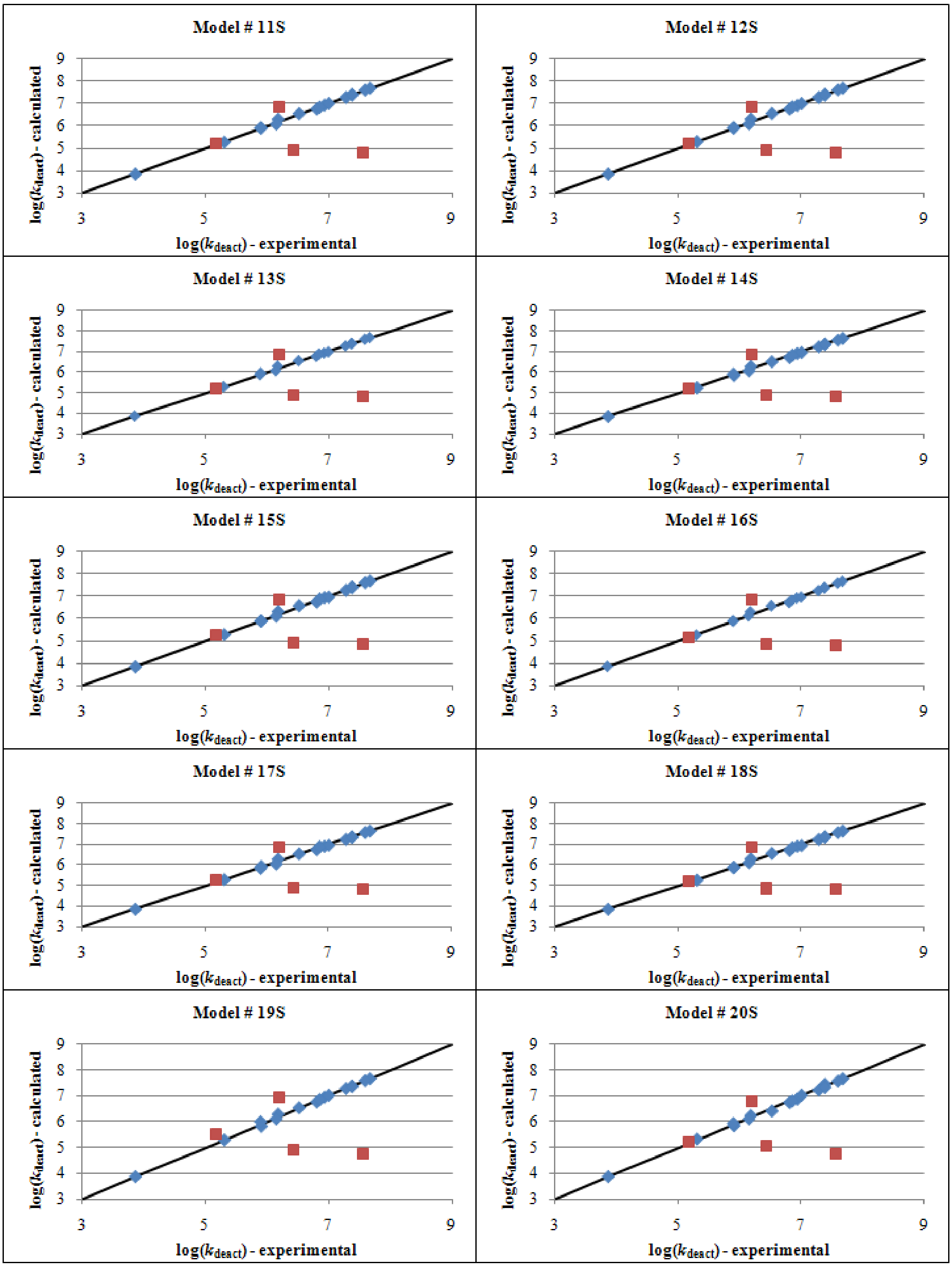
Model # 11S
Model # 12S
Model # 13S
Model # 14S
Model # 15S
Model # 16S
Model # 17S
Model # 18S
Model # 19S
Model # 20S
log(k_{deact}) - calculated
log(k_{deact}) - experimental

Figure 6S. Calculated *vs*. experimental $\log(k_{deact})$ values for Cu(II) deactivators obtained by genetic function approximation analysis with linear splines. Training and test sets are represented by the symbols "♦" and "■", respectively.

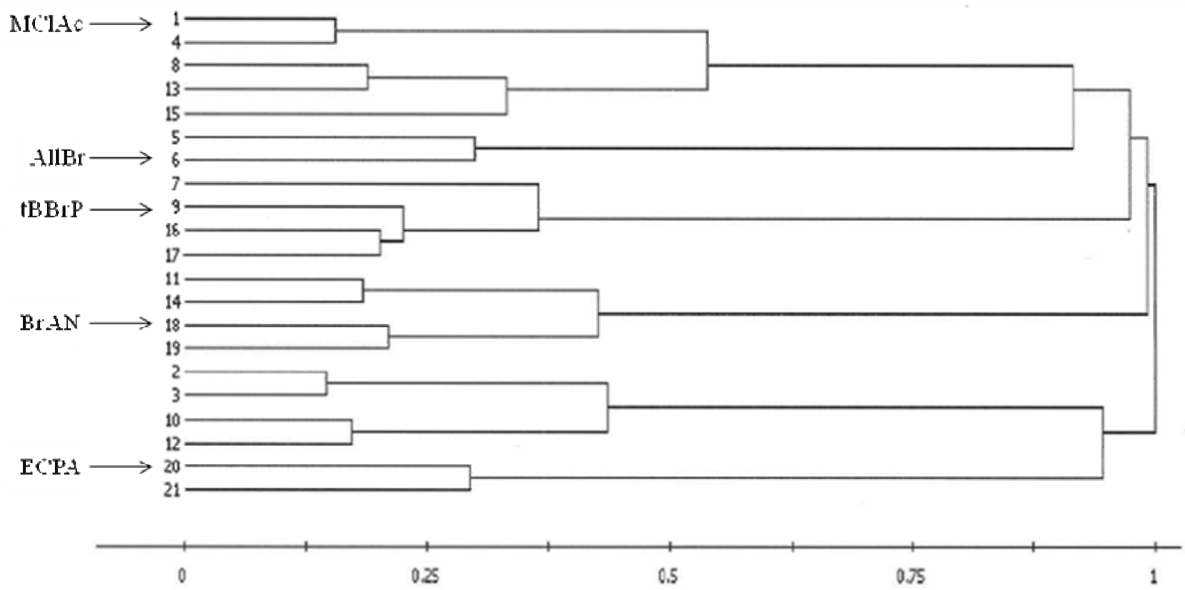

Figure 7S. Dendrogram resulting from HCA carried out on the first 6 principal components obtained by subjecting the molecular descriptors of alkyl halide initiators to PCA.

	Model	Friedman's LOF	R^2	Adjusted R^2	Cross-validated R^2	SOR F-value	Critical SOR F-value (95%)
21S	$-\log(k_{act}) = -17\times10^{-3}(I_X) - 7.9\times10^{-3}(\langle I_X-2.2\times10^{2}\rangle) - 3.0(\langle CN-0.59\rangle) + 3.1(\langle \kappa_1-9.0\rangle) - 0.54(\langle 8.1-\kappa_1\rangle) + 1.4(\langle 5.9-{}^{0}\chi^{v}\rangle) - 66\times10^{-3}(\langle 1.3\times10^{2}-MV\rangle) - 27(\langle -65\times10^{-3}-LUMO\rangle) + 6.1$	18.3×10^{-4}	1	1	-2.39	1.70×10^{4}	3.45

22S	$-\log(k_{act}) = - 17\times10^{-3}(I_X) - 7.9\times10^{-3}(\langle I_X-2.2\times10^2\rangle) + 3.1(\langle 0.39-CN\rangle) + 3.1(\langle \kappa_1-9.0\rangle) - 0.54(\langle 8.1-\kappa_1\rangle) + 1.4(\langle 5.9-{}^0\chi^v\rangle) - 66\times10^{-3}(\langle 1.3\times10^2-MV\rangle) - 27(\langle -65\times10^{-3}-LUMO\rangle) + 4.9$	18.3×10^{-4}	1	1	-2.39	1.70×10^4	3.45
23S	$-\log(k_{act}) = - 1.2(CN) - 17\times10^{-3}(I_X) - 7.9\times10^{-3}(\langle I_X-2.2\times10^2\rangle) + 3.1(\langle \kappa_1-9.0\rangle) - 0.54(\langle 8.1-\kappa_1\rangle) + 1.4(\langle 5.9-{}^0\chi^v\rangle) - 66\times10^{-3}(\langle 1.3\times10^2-MV\rangle) - 27(\langle -65\times10^{-3}-LUMO\rangle) + 6.1$	18.3×10^{-4}	1	1	-2.39	1.70×10^4	3.45
24S	$-\log(k_{act}) = - 1.2(CN) - 17\times10^{-3}(I_X) - 7.9\times10^{-3}(\langle I_X-2.2\times10^2\rangle) + 42(\langle RoG-3.2\rangle) - 0.54(\langle 8.1-\kappa_1\rangle) + 1.4(\langle 5.9-{}^0\chi^v\rangle) - 66\times10^{-3}(\langle 1.3\times10^2-MV\rangle) - 27(\langle -65\times10^{-3}-LUMO\rangle) + 6.1$	18.6×10^{-4}	1	1	0.997	1.67×10^4	3.45
25S	$-\log(k_{act}) = - 1.2(CN) - 17\times10^{-3}(I_X) - 7.9\times10^{-3}(\langle I_X-2.2\times10^2\rangle) + 0.71(\langle MR-45\rangle) - 0.54(\langle 8.1-\kappa_1\rangle) + 1.4(\langle 5.9-{}^0\chi^v\rangle) - 66\times10^{-3}(\langle 1.3\times10^2-MV\rangle) - 27(\langle -65\times10^{-3}-LUMO\rangle) + 6.1$	18.6×10^{-4}	1	1	1	1.67×10^4	3.45
26S	$-\log(k_{act}) = - 17\times10^{-3}(I_X) - 7.9\times10^{-3}(\langle I_X-2.2\times10^2\rangle) - 2.8(\langle CN-0.57\rangle) + 4.7(\langle {}^0\chi^v-7.6\rangle) + 1.4(\langle 5.9-{}^0\chi^v\rangle) - 0.54(\langle 8.1-\kappa_1\rangle) - 66\times10^{-3}(\langle 1.3\times10^2-MV\rangle) - 27(\langle -65\times10^{-3}-LUMO\rangle) + 6.1$	18.6×10^{-4}	1	1	0.998	1.67×10^4	3.45
27S	$-\log(k_{act}) = - 1.2(CN) - 17\times10^{-3}(I_X) - 7.9\times10^{-3}(\langle I_X-2.2\times10^2\rangle) + 4.7(\langle {}^0\chi^v-7.6\rangle) + 1.4(\langle 5.9-{}^0\chi^v\rangle) - 0.54(\langle 8.1-\kappa_1\rangle) - 66\times10^{-3}(\langle 1.3\times10^2-MV\rangle) - 27(\langle -65\times10^{-3}-LUMO\rangle) + 6.1$	18.6×10^{-4}	1	1	0.999	1.67×10^4	3.45

28S	$-\log(k_{act}) = -17\times10^{-3}(I_X) - 7.9\times10^{-3}(\langle I_X-2.2\times10^{2}\rangle) - 2.5(\langle CN-0.52\rangle) + 42(\langle RoG-3.2\rangle) - 0.54(\langle 8.1-\kappa_1\rangle) + 1.4(\langle 5.9-{}^{0}\chi^{v}\rangle) - 66\times10^{-3}(\langle 1.3\times10^{2}-MV\rangle) - 27(\langle -65\times10^{-3}-LUMO\rangle) + 6.1$	18.6×10^{-4}	1	1	0.963	1.67×10^{4}	3.45
29S	$-\log(k_{act}) = -17\times10^{-3}(I_X) - 7.9\times10^{-3}(\langle I_X-2.2\times10^{2}\rangle) + 3.1(\langle 0.39-CN\rangle) + 42(\langle RoG-3.2\rangle) - 0.54(\langle 8.1-\kappa_1\rangle) + 1.4(\langle 5.9-{}^{0}\chi^{v}\rangle) - 66\times10^{-3}(\langle 1.3\times10^{2}-MV\rangle) - 27(\langle -65\times10^{-3}-LUMO\rangle) + 4.9$	18.6×10^{-4}	1	1	0.999	1.67×10^{4}	3.45
30S	$-\log(k_{act}) = -17\times10^{-3}(I_X) - 7.9\times10^{-3}(\langle I_X-2.2\times10^{2}\rangle) - 2.5(\langle CN-0.52\rangle) + 5.2(\langle {}^{3}\chi_{path}-2.8\rangle) - 0.54(\langle 8.1-\kappa_1\rangle) + 1.4(\langle 5.9-{}^{0}\chi^{v}\rangle) - 66\times10^{-3}(\langle 1.3\times10^{2}-MV\rangle) - 27(\langle -65\times10^{-3}-LUMO\rangle) + 6.1$	18.6×10^{-4}	1	1	0.969	1.67×10^{4}	3.45

Table 3S. Top 10 models and relative statistical analysis for $\log(k_{act})$ of alkyl halide initiators obtained with genetic function approximation algorithm with linear splines. The models are in order of increasing Friedman's LOF values.

	Model	Friedman's LOF	R^2	Adjusted R^2	Cross-validated R^2	SOR F-value	Critical SOR F-value (95%)
31S	$-\log(K_{ATRP}) = -1.9(CN) - 9.1\times10^{-3}(I_X) - 20(\langle J_X-3.0\rangle) + 4.8(\langle J_Y-2.7\rangle) - 41(\langle \delta_Z+0.68\rangle) + 20(\langle 0.54-\delta_Z\rangle) - 60(\langle 0.96-\delta_Z\rangle) + 1.3\times10^{2}$	34.9×10^{-3}	0.999	0.998	0.994	934	3.45

	(❬C-X-2.3❭) + 82						
32S	-log(K_{ATRP}) = - 9.1×10^{-3}(I$_X$) - 6.3(❬CN-0.70❭) - 20(❬J$_X$-3.0❭) + 4.8(❬J$_Y$-2.7❭) - 41(❬δ$_Z$+0.68❭) + 20(❬0.54-δ$_Z$❭) - 60(❬0.96-δ$_Z$❭) + 1.3×10^2(❬C-X-2.3❭) + 82	34.9×10^{-3}	0.999	0.998	0.994	934	3.45
33S	-log(K_{ATRP}) = - 9.1×10^{-3}(I$_X$) + 4.8(❬0.39-CN❭) - 19(❬J$_X$-3.0❭) + 5.2(❬J$_Y$-2.7❭) - 37(❬δ$_Z$+0.68❭) + 18(❬0.54-δ$_Z$❭) - 53(❬0.96-δ$_Z$❭) + 1.3×10^2(❬C-X-2.3❭) + 73	34.9×10^{-3}	0.999	0.998	0.994	934	3.45
34S	-log(K_{ATRP}) = -2.0(CN) - 9.1×10^{-3}(I$_X$) + 34(❬J$_X$-3.2❭) - 22(❬J$_X$-3.5❭) - 26(❬J$_X$-3.1❭) + 4.2(❬J$_Y$-2.7❭) + 19(❬MD-1.7❭) - 1.2(❬δ$_Z$+0.66❭) + 9.4	37.2×10^{-3}	0.999	0.998	0.606	874	3.45
35S	-log(K_{ATRP}) = - 9.1×10^{-3}(I$_X$) - 5.6(❬CN-0.64❭) + 34(❬J$_X$-3.2❭) - 22(❬J$_X$-3.5❭) - 26(❬J$_X$-3.1❭) + 4.2(❬J$_Y$-2.7❭) - 1.2(❬δ$_Z$+0.66❭) + 8.5×10^{-4}(❬-4.6×10^3-TE❭) + 9.4	37.2×10^{-3}	0.999	0.998	-1	874	3.45
36S	-log(K_{ATRP}) = - 9.1×10^{-3}(I$_X$) - 5.6(❬CN-0.64❭) + 34(❬J$_X$-3.2❭) - 22(❬J$_X$-3.5❭) - 26(❬J$_X$-3.1❭) + 4.2(❬J$_Y$-2.7❭) - 1.2(❬δ$_Z$+0.66❭) + 1.5×10^2(❬C-X-2.3❭) + 9.4	37.2×10^{-3}	0.999	0.998	0.997	874	3.45
37S	-log(K_{ATRP}) = - 9.1×10^{-3}(I$_X$) - 5.6(❬CN-0.64❭) + 34(❬J$_X$-3.2❭) - 22(❬J$_X$-3.5❭) - 26(❬J$_X$-3.1❭) + 4.2(❬J$_Y$-2.7❭) + 19(❬MD-1.7❭) - 1.2(❬δ$_Z$+0.66❭) + 9.4	37.2×10^{-3}	0.999	0.998	0.823	874	3.45

38S	$-\log(K_{ATRP}) = -2.0(CN) - 9.1\times10^{-3}(I_X) + 34(\langle J_X-3.2\rangle) - 22(\langle J_X-3.5\rangle) - 26(\langle J_X-3.1\rangle) + 4.2(\langle J_Y-2.7\rangle) - 1.2(\langle \delta_Z+0.66\rangle) + 1.5\times10^{2}(\langle C-X-2.3\rangle) + 9.4$	37.2×10^{-3}	0.999	0.998	0.606	874	3.45
39S	$-\log(K_{ATRP}) = -2.0(CN) - 9.1\times10^{-3}(I_X) + 34(\langle J_X-3.2\rangle) - 22(\langle J_X-3.5\rangle) - 26(\langle J_X-3.1\rangle) + 4.2(\langle J_Y-2.7\rangle) - 1.2(\langle \delta_Z+0.66\rangle) + 8.5\times10^{-4}(\langle -4.6\times10^{3}-TE\rangle) + 9.4$	37.2×10^{-3}	0.999	0.998	0.487	874	3.45
40S	$-\log(K_{ATRP}) = -9.1\times10^{-3}(I_X) - 5.6(\langle CN-0.64\rangle) + 34(\langle J_X-3.2\rangle) - 22(\langle J_X-3.5\rangle) - 26(\langle J_X-3.1\rangle) + 4.2(\langle J_Y-2.7\rangle) + 12(\langle MD-1.7\rangle) - 1.2(\langle \delta_Z+0.66\rangle) + 9.4$	37.2×10^{-3}	0.999	0.998	1.01×10^{5}	874	3.45

Table 4S. Top 10 models and relative statistical analysis for $\log(K_{ATRP})$ of alkyl halide initiators obtained with genetic function approximation algorithm with linear splines. The models are in order of increasing Friedman's LOF values.

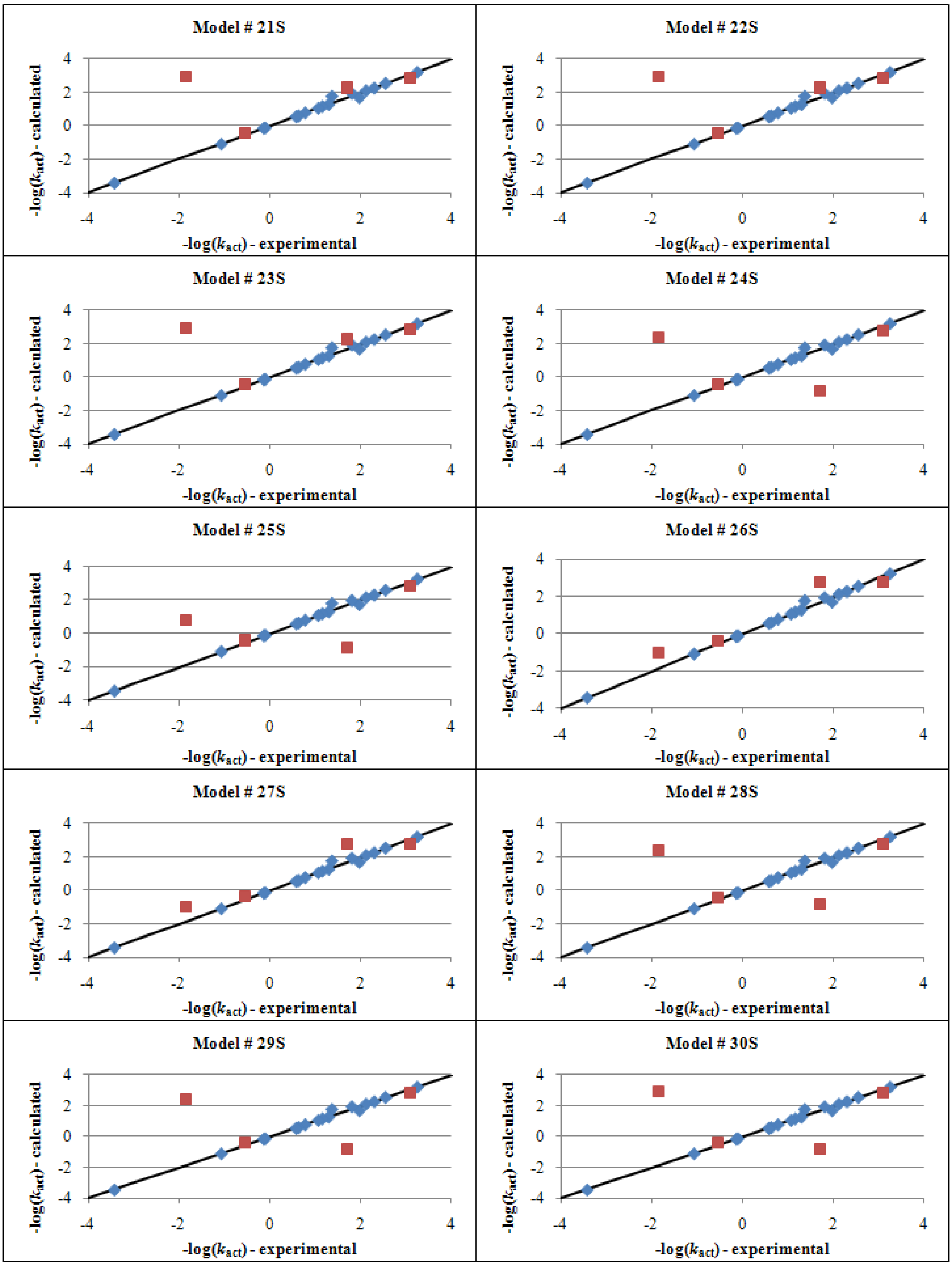
Model # 21S
Model # 22S
Model # 23S
Model # 24S
Model # 25S
Model # 26S
Model # 27S
Model # 28S
Model # 29S
Model # 30S
-log(kact) - calculated
-log(kact) - experimental
4
2
0
-2
-4

Figure 8S. Calculated *vs*. experimental log(k_{act}) values for alkyl halide initiators obtained by genetic function approximation analysis with linear splines. Training and test sets are represented by the symbols "♦" and "■", respectively.

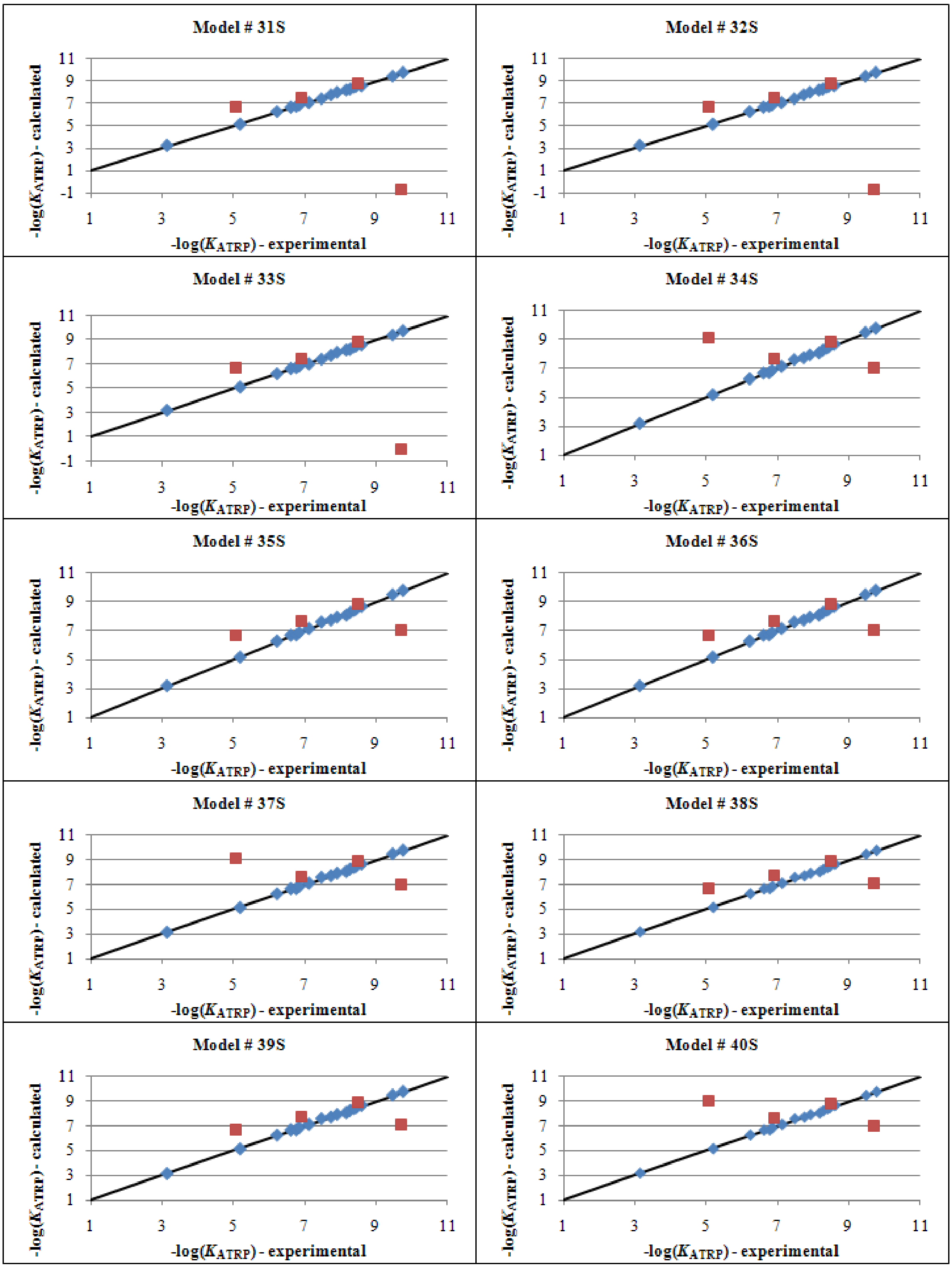
Model # 31S
Model # 32S
Model # 33S
Model # 34S
Model # 35S
Model # 36S
Model # 37S
Model # 38S
Model # 39S
Model # 40S
-log(KATRP) - calculated
-log(KATRP) - experimental

Figure 9S. Calculated *vs*. experimental log(K_{ATRP}) values for alkyl halide initiators obtained by genetic function approximation analysis with linear splines. Training and test sets are represented by the symbols "♦" and "■", respectively.

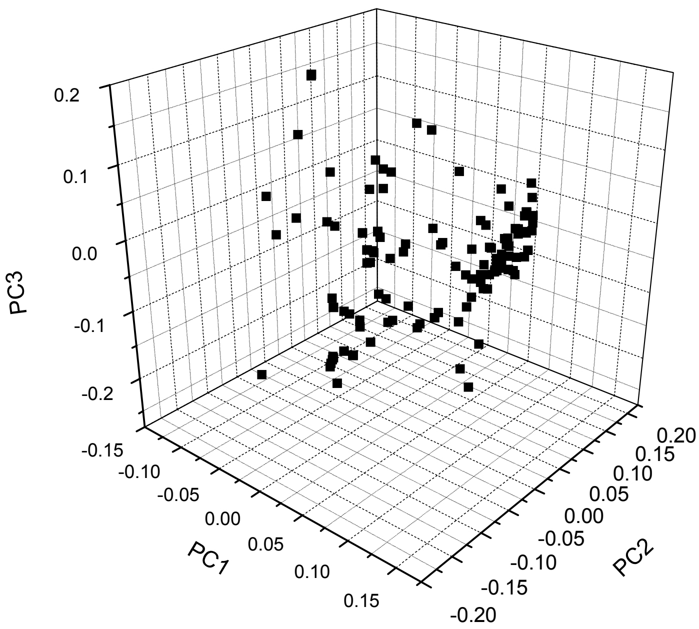

Figure 10S. Loading plot PC1 *vs.* PC2 *vs.* PC3 for the molecular descriptors of alkyl halide initiators.